Radiative neutrino mass generation through vectorlike quarks

K. S. Babu and J. Julio

Phys. Rev. D **85**, 073005 — Published 5 April 2012
DOI: 10.1103/PhysRevD.85.073005

OSU-HEP-11-10

Radiative Neutrino Mass Generation through Vector–like Quarks

K. S. Babu[*] *and J. Julio*[†]

Department of Physics
Oklahoma State University
Stillwater, OK 74078, USA

Abstract

A new model of radiative neutrino masses generated via two–loop diagrams is proposed involving a charge 2/3 vector–like quark and a doublet of leptoquark scalars. This model predicts one of the neutrinos to be massless and admits both the normal and inverted neutrino mass hierarchies with correlated predictions for $\ell_i \to \ell_j + \gamma$ branching ratios. New contributions to CP violation in $B_s^0 - \overline{B_s^0}$ mixing arise in the model through leptoquark box diagrams, which can explain the anomalous dimuon events reported by the DØ collaboration. These leptoquarks, with masses below 500 GeV, also provide a natural resolution to the apparent discrepancy in the measured values of the CP violation parameters $\sin 2\beta$ and ϵ_K.

[*]Email: babu@okstate.edu
[†]julio.julio@okstate.edu

1 Introduction

Neutrinos must have tiny masses, so that different flavors can oscillate among one another, as observed in experiments. An elegant and natural way to generate the tiny masses is through the dimension–five lepton number violating operator $\mathcal{L} = \mathcal{O}_1/M$ where [1]

$$\mathcal{O}_1 = L^i L^j H^k H^l \,\epsilon_{ik}\,\epsilon_{jl}\ . \tag{1}$$

Here L is the lepton doublet and H the Higgs doublet, with $i, j = 1, 2$ being $SU(2)_L$ indices. The suppression by an inverse power of M, which can be much greater than the weak scale, explains the smallness of neutrino mass, which is given by $m_\nu \sim v^2/M$, with $\langle H^0 \rangle \equiv v \simeq 174$ GeV being the Higgs boson vacuum expectation value (VEV). Operator $\mathcal{O}_1$ is naturally realized through the seesaw mechanism wherein right–handed neutrinos, which are singlets of the standard model (SM) gauge group with large Majorana masses, are integrated out [2]. The effective mass scale M should be of order 10^{14} GeV in order to generate neutrino masses of order 0.1 eV, as indicated by neutrino oscillation experiments. Such a large scale of M would however make this mechanism difficult to test directly in experiments such as the ones pursued at the Large Hadron Collider.

An alternative method for inducing naturally small neutrino masses is the radiative mass generation mechanism [3–7]. This scheme posits that the dimension 5 operator $\mathcal{O}_1$ of Eq. (1) is absent, or is highly suppressed, so that neutrino masses remain zero at the tree level. Lepton number violation arises through effective operators with dimension $d > 5$, typically containing charged fermions as well as the neutrino fields. These operators can be converted to neutrino mass, but only through loop diagrams, wherein all charged fermions are annihilated. The induced neutrino masses are naturally small, even when new particles needed to generate the $d > 5$ lepton number violating operators have masses in the TeV range, owing to chirality and loop suppression factors.

The simplest set of operators carrying two units of lepton number appropriate for small Majorana neutrino mass generation, in the absence of $\mathcal{O}_1$ of Eq. (1), is of dimension seven. There are six such $d = 7$ operators [8]:

$$\begin{aligned}
\mathcal{O}_2 &= L^i L^j L^k e^c H^l \,\epsilon_{ij}\epsilon_{kl} \\
\mathcal{O}_3 &= \{L^i L^j Q^k d^c H^l \,\epsilon_{ij}\epsilon_{kl},\ L^i L^j Q^k d^c H^l \,\epsilon_{ik}\epsilon_{jl}\} \\
\mathcal{O}_4 &= \{L^i L^j \bar{Q}_i \bar{u}^c H^k \,\epsilon_{jk},\ L^i L^j \bar{Q}_k \bar{u}^c H^k \,\epsilon_{ij}\} \\
\mathcal{O}_8 &= L^i \bar{e}^c \bar{u}^c d^c H^j \,\epsilon_{ij}\ .
\end{aligned} \tag{2}$$

Here the generation and color indices have been suppressed. Q, L denote left-handed quark and lepton doublets, while u^c, d^c, e^c denote left-handed anti-quark and anti-lepton singlets of the standard model. A full list of $\Delta L = 2$ effective operators through $d = 11$ is given in Ref. [8]. Among the $d = 7$ operators of Eq. (2), $\mathcal{O}_2$ is perhaps the simplest, which can be induced when the scalar spectrum of the standard model is extended to include a second Higgs boson doublet and a charged singlet scalar field $h^{\pm}$. This is the well–studied Zee model of neutrino masses [3]. In its simplest version, with natural flavor conservation in the Higgs sector, this model predicts vanishing diagonal elements of the neutrino mass matrix [3, 9], which is now excluded by neutrino oscillation data [10].

A second widely studied model of radiative neutrino mass generation [6, 7] has a purely leptonic effective $d = 9$ operator, $\mathcal{O}_9 = L^i L^j L^k e^c L^l e^c \, \epsilon_{ij} \epsilon_{kl}$, suppressed by M^{-5}. Here neutrino masses are induced via two–loop diagrams. This operator can be obtained when the standard model is extended to include a singly charged (h^+) scalar and a doubly charged (k^{++}) scalar. The resulting model fits the neutrino oscillation data well, and also predicts a host of leptonic flavor violation processes, some of which within reach of ongoing and next generation experiments [11]. Operator $\mathcal{O}_8$ of Eq. (2) is best induced by scalar leptoquarks, as recently shown by us in Ref. [12]. This model leads to consistent neutrino phenomenology and interesting flavor effects in both the quark and the lepton sectors [12]. For discussions of models based on other operators, see Ref. [8, 13, 14].

Operator $\mathcal{O}_3$ of Eq. (2) is the main focus of this paper. It has two different $SU(2)_L$ contractions possible, as shown in Eq. (2). These operators arise in supersymmetric models with R–parity violation. The superpotential couplings $W' \supset \lambda L L e^c + \lambda' Q L d^c$ would generate $\mathcal{O}_3$ once the SUSY particles are integrated out [5, 15]. The QLd^c term would induce the second contraction of $\mathcal{O}_3$ in Eq. (2), the LLe^c term would induce $\mathcal{O}_2$, while the product of QLd^c and LLe^c would induce the first contraction of $\mathcal{O}_3$. There is an important difference in the first and second $SU(2)_L$ contractions of $\mathcal{O}_3$: In the second contraction, neutrino masses are induced at the one–loop, while in the first contraction, they arise only at the two–loop level. (In the second contraction, two neutrino fields appear, while the first has one neutrino field and a charged lepton field, which must be annihilated to convert this operator to neutrino mass.) The focus of this paper is models which induce the first contraction of $\mathcal{O}_3$, without inducing other operators that lead to one–loop neutrino masses. SUSY with R–parity violation does not fit this requirement, as $\mathcal{O}_2$ and/or the second contraction of $\mathcal{O}_3$ are also induced there. The simplest possibility we have found is to add a vector–like charge 2/3 iso–singlet quark to the SM, along with a doublet of leptoquark scalars. The induced neutrino mass in such a model would be of the form

$$m_\nu \sim \frac{f g h \lambda_b}{(16\pi^2)^2} \, \frac{v^2}{M} \, , \tag{3}$$

where f, g, h are dimensionless Yukawa couplings, $\lambda_b = m_b/v$ is the b–quark Yukawa coupling, and M stands for an effective mass of the vector–like quark/leptoquark. For $f \sim g \sim h \sim 10^{-2}$, the mass scale M should be of order TeV, in order to generate $m_\nu \sim 0.1$ eV. It is, however, evident from Eq. (3) that M can be as large as about 10^8 GeV, when f, g, h are of order one. There are several reasons for considering low values of M, first and foremost being direct tests of the vector quark and the leptoquarks at the LHC. There are hints of new physics in the B meson system, which can be explained by the new leptoquark scalars and/or the vector–like quark of the present model. The DØ collaboration has reported an excess in the same sign di-muon asymmetry in B decays [16], which may be a hint for new CP violation in $B_s^0 - \overline{B_s^0}$ mixing. There has also been a tension in the determinations of the CP asymmetry parameters $\sin 2\beta$ in the B meson system and ϵ_K in the Kaon system, which may need new physics [17, 18]. The present model, with leptoquark masses below a TeV, can explain these anomalies. Furthermore, when this model is eventually embedded in a supersymmetric framework, M of Eq. (3) will have to be close to the SUSY breaking scale, owing to the SUSY non-renormalization theorem, which requires that all loop diagrams that generate neutrino masses cancel in the supersymmetric limit.

The rest of the paper is organized as follows. In Sec. 2 we present the model leading to the two-loop neutrino mass generation via $\mathcal{O}_3$, the first contraction of Eq. (2). In Sec. 3 we obtain the experimental constraints on the model parameters arising from rare process in the quark as well as lepton sectors. Here we show how the proposed model explains the discrepancy observed by DØ in the CP asymmetry of the B_s system. New contributions to the CP violating decay $B_d^0 \to J/\psi K_S$ are shown to be of the right magnitude to explain the apparent tension between $\sin 2\beta$ and ϵ_K determinations. In Sec. 3 we also evaluate the rate for neutrinoless double beta decay induced via the vector-scalar exchange mechanism [19]. Finally, we give our conclusions in Sec. 4.

2 Radiative neutrino mass model with vector–like quarks

We wish to generate the operator $(L \cdot L)(Q \cdot H)d^c$ in a renormalizable theory. Here and in discussions that follow we use a compact dot product notation for $SU(2)_L$ contraction: $L \cdot L = L^i L^j \epsilon_{ij}$, $Q \cdot H = Q^i H^j \epsilon_{ij}$, etc. The simplest way to generate this operator, without inducing other operators that generate neutrino masses at one loop, is by integrating out a charge 2/3 iso-singlet vector–like quark, and a doublet of scalar leptoquarks. These fields transform under $SU(3)_c \times SU(2)_L \times U(1)_Y$ as

$$\text{Fermions}: \quad U(3,1,2/3) + U^c(3^*,1,-2/3), \qquad \text{Scalars}: \Omega(3,2,1/6) \equiv \begin{pmatrix} \omega^{2/3} \\ \omega^{-1/3} \end{pmatrix}. \quad (4)$$

These particles will have new Yukawa interactions with the SM fermions as well as gauge invariant masses given by

$$\mathcal{L}^{\text{new}} = \left(g_{ij} d_j^c L_i \cdot \Omega \; + \; h_i U L_i \cdot \tilde{\Omega} \; - \; f_i U^c Q_i \cdot H \; + \; \text{h.c.} \right) - M U U^c, \quad (5)$$

where $\tilde{\Omega} \equiv i\tau^2 \Omega^*$. Here the dots indicates $SU(2)_L$ contraction, as mentioned earlier, and we use indices i, j to denote generations. Possible mass terms $m_i \, u_i^c U$, not shown in Eq. (5), can be rotated away by field redefinitions. The simultaneous presence of the interaction terms g_{ij}, h_i, f_i would lead to lepton number violation by two units, a necessary condition for neutrino mass generation.

We should also specify the scalar interactions that couple the leptoquark Ω with the SM Higgs doublet H. There is a single non-trivial quartic coupling between these two fields:

$$\mathcal{L}_{\rm quart}^{\rm new} = \lambda\, |\Omega \cdot H|^2 \tag{6}$$

When the neutral component of the SM Higgs doublet H^0 acquires a VEV, this quartic coupling will generate a mass splitting between $\omega^{2/3}$ and $\omega^{-1/3}$ leptoquarks:

$$M^2_{\omega^{-1/3}} \equiv M_1^2, \quad M^2_{\omega^{2/3}} \equiv M_2^2 = M_1^2 - \lambda v^2, \tag{7}$$

where $v \equiv \sqrt{2} m_W/g \simeq 174$ GeV.

The mass matrix for the charge 2/3 quarks, including U, U^c fields, that follows from Eq. (5) has the form

$$M_u = \begin{pmatrix} Y_u v & 0 \\ f v & M \end{pmatrix}, \tag{8}$$

where (u_i^c, U^c) multiply on the left and (u_i, U) multiply on the right. Here Y_u is a 3×3 matrix, f is a 1×3 row vector, and 0 stands for the 3×1 null column vector. This mass matrix can be diagonalized by a biunitary transformation

$$M_u^{\rm d} = U M_u V^\dagger \tag{9}$$

where U, V are 4×4 unitary matrices. Without loss of generality we choose a basis where the 3×3 matrices for the down quarks and charged leptons are diagonal. Thus, the CKM matrix will be the 4×3 sub-matrix of the 4×4 matrix V. The charged current interactions of the quarks, therefore, become

$$\mathcal{L}^{cc,q}_{\rm vector} = \frac{g}{2\sqrt{2}}\, \overline{u}_\alpha V_{\alpha i} \gamma^\mu (1-\gamma_5) d_i W^+_\mu + {\rm h.c.}, \tag{10}$$

$$\mathcal{L}^{cc,q}_{\rm scalar} = \frac{g}{2\sqrt{2} m_W}\, \overline{u}_\alpha \left[(M_u^d)_\alpha V_{\alpha i} (1-\gamma_5) - V_{\alpha i} (M_d)_i (1+\gamma_5) \right] d_i\, H^+ \; + \; {\rm h.c.} \tag{11}$$

The Greek indices $\alpha, \beta = 1-4$ label generations in the up–quark sector ($u_1 = u,\ u_2 = c,\ u_3 = t,\ u_4 = t'$), while the Latin indices $i, j = 1-3$ label generations in the down–quark and lepton sectors. Introduction of vector-like quarks U, U^c to the SM spectrum will induce flavor changing neutral currents (FCNC) in the charge 2/3 quark sector, which are given by

$$\mathcal{L}^{nc,q}_{\rm vector} = \frac{g}{4\cos\theta_W}\, \overline{u}_\alpha \left[\delta_{\alpha\beta} \gamma^\mu \left(1 - \tfrac{8}{3}\sin^2\theta_W - \gamma_5\right) - V_{\alpha 4} V^*_{\beta 4} \gamma^\mu (1-\gamma_5) \right] u_\beta Z_\mu, \tag{12}$$

$$\mathcal{L}^{nc,q}_{\rm scalar} = \frac{g}{2\sqrt{2} m_W}\, \overline{u}_\alpha (M_u)_\alpha V_{\alpha j} V^*_{\beta j} (1-\gamma_5) u_\beta H^0 + {\rm h.c.} \tag{13}$$

These interactions can generate tree-level $D^0 - \overline{D^0}$ mixing, which will strongly constrain the product $|V_{14}V_{24}|$. This issue will be discussed in the next section.

The 4×4 unitary matrix V can be parameterized as [20]

$$V = \begin{pmatrix} c_{12}c_{13}c_{14} & c_{13}c_{14}s_{12} & c_{14}s_{13}e^{-i\delta_{13}} & s_{14}e^{-i\delta_{14}} \\ \begin{matrix} -c_{23}c_{24}s_{12} - c_{12}c_{24}s_{13}s_{23}e^{i\delta_{13}} \\ -c_{12}c_{13}s_{14}s_{24}e^{i(\delta_{14}-\delta_{24})} \end{matrix} & \begin{matrix} c_{12}c_{23}c_{24} - c_{24}s_{12}s_{13}s_{23}e^{i\delta_{13}} \\ -c_{13}s_{12}s_{14}s_{24}e^{i(\delta_{14}-\delta_{24})} \end{matrix} & \begin{matrix} c_{13}c_{24}s_{23} \\ -s_{13}s_{14}s_{24}e^{-i(\delta_{13}+\delta_{24}-\delta_{14})} \end{matrix} & c_{14}s_{24}e^{-i\delta_{24}} \\ \begin{matrix} c_{34}s_{12}s_{23} - c_{12}c_{23}c_{34}s_{13}e^{i\delta_{13}} \\ -c_{12}c_{13}c_{24}s_{14}s_{34}e^{i\delta_{14}} \\ +c_{23}s_{12}s_{24}s_{34}e^{i\delta_{24}} \\ +c_{12}s_{23}s_{24}s_{34}s_{13}e^{i(\delta_{13}+\delta_{24})} \end{matrix} & \begin{matrix} -c_{12}c_{34}s_{23} - c_{23}c_{34}s_{12}s_{13}e^{i\delta_{13}} \\ -c_{12}c_{23}s_{24}s_{34}e^{i\delta_{24}} \\ -c_{13}c_{24}s_{12}s_{14}s_{34}e^{i\delta_{14}} \\ +s_{12}s_{23}s_{24}s_{34}s_{13}e^{i(\delta_{13}+\delta_{24})} \end{matrix} & \begin{matrix} c_{13}c_{23}c_{34} \\ -c_{13}s_{23}s_{24}s_{34}e^{i\delta_{24}} \\ -c_{24}s_{13}s_{14}s_{34}e^{i(\delta_{14}-\delta_{13})} \end{matrix} & c_{14}c_{24}s_{34} \\ \begin{matrix} -c_{12}c_{13}c_{24}c_{34}s_{14}e^{i\delta_{14}} \\ +c_{12}c_{23}s_{13}s_{34}e^{i\delta_{13}} \\ +c_{23}c_{34}s_{12}s_{24}e^{i\delta_{24}} - s_{12}s_{23}s_{34} \\ +c_{12}c_{34}s_{13}s_{23}s_{24}e^{i(\delta_{13}+\delta_{24})} \end{matrix} & \begin{matrix} -c_{12}c_{23}c_{34}s_{24}e^{i\delta_{24}} + c_{12}s_{23}s_{34} \\ -c_{13}c_{24}c_{34}s_{12}s_{14}e^{i\delta_{14}} \\ +c_{23}s_{12}s_{13}s_{34}e^{i\delta_{13}} \\ +c_{34}s_{12}s_{13}s_{23}s_{24}e^{i(\delta_{13}+\delta_{24})} \end{matrix} & \begin{matrix} -c_{13}c_{23}s_{34} \\ -c_{13}c_{34}s_{23}s_{24}e^{i\delta_{24}} \\ -c_{24}c_{34}s_{13}s_{14}e^{i(\delta_{14}-\delta_{13})} \end{matrix} & c_{14}c_{24}c_{34} \end{pmatrix}, \tag{14}$$

where $s_{\alpha\beta} \equiv \sin\theta_{\alpha\beta},\ c_{\alpha\beta} \equiv \cos\theta_{\alpha\beta}$. The CKM mixing matrix elements $V_{\alpha i}$ are the elements of the 4×3 sub-matrix of V. In terms of the fermion mass eigenstates, the Yukawa interactions of Eq. (5) can be written as

$$\begin{aligned} \mathcal{L}_Y^{\text{new}} &= \bar{d}_j\ (g^T)_{ji}\ \frac{(1-\gamma_5)}{2}\ \left(\nu_i\omega^{-1/3} - \ell_i\omega^{2/3}\right) \\ &- \left(\nu_i^T C^T \omega^{-2/3} + \ell_i^T C^T \omega^{1/3}\right) h_i\ V_{\alpha 4}^* \frac{(1-\gamma_5)}{2} u_\alpha + \text{h.c.} \end{aligned} \tag{15}$$

which will be used in our calculations.

2.1 Two–loop neutrino masses

By combining the interactions given in Eqs. (6), (10), (11) and (15), one can construct diagrams generating neutrino masses. These diagrams arise at the two–loop level, and are shown in Fig. 1. We have evaluated these diagrams in general R_ξ gauge, so the unphysical Goldstone mode H^+ also appears in this set. A non-trivial check of the calculation is the gauge independence of the induced neutrino mass, which we shall show explicitly. Since the external neutrinos are Majorana particles, there is another set of diagrams identical to the ones in Fig. 1, but with all internal particles replaced by their charge conjugates. The sum of these diagrams would make the neutrino mass matrix symmetric in flavor space.

The induced neutrino mass matrix is proportional to the down quark mass matrix, since these diagrams make use of the SM charged currents, which require a chirality flip for the d^c fields. This is explicitly shown in Fig. 1. The neutrino mass matrix, therefore, can be

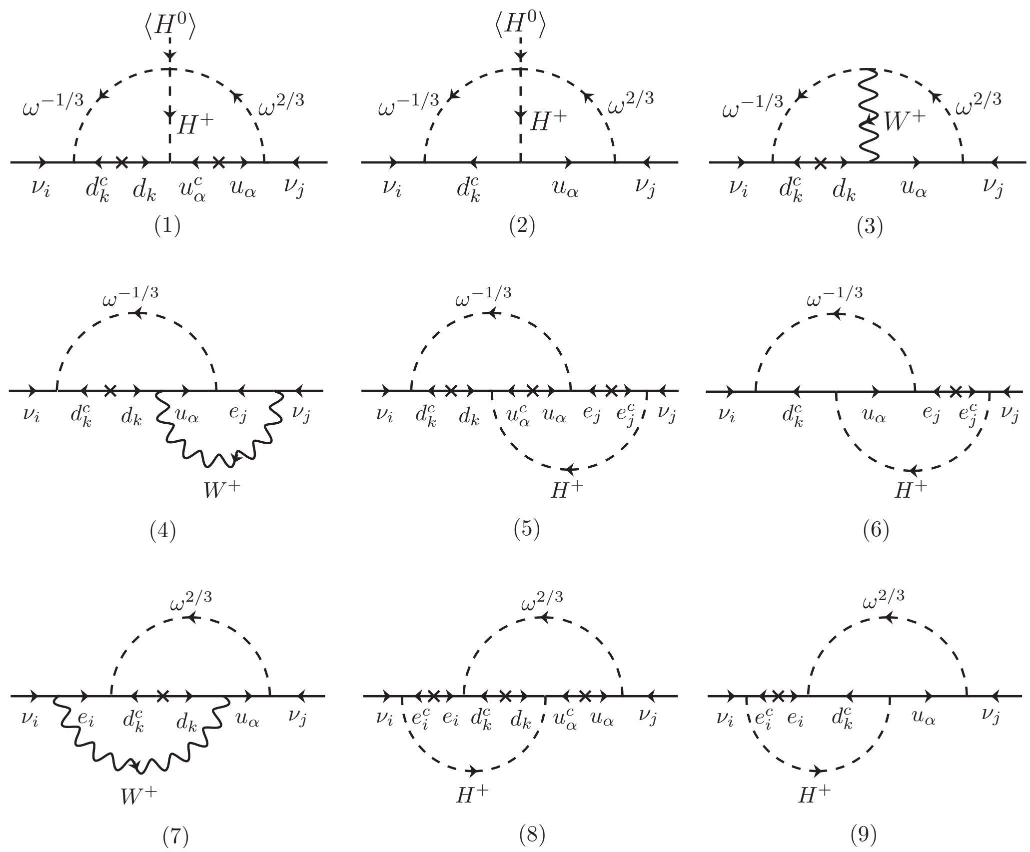

Figure 1: Two-loop diagrams leading to finite neutrino masses in general R_ξ gauge.

written as

$$(M_\nu)_{ij} = \frac{3}{2} g^2 m_b \left[h_i (V^\dagger)_{4\alpha} V_{\alpha k} (D_d)_k (g^T)_{kj} \hat{I}_{\alpha k i j} + g_{ik} (D_d)_k (V^T)_{k\alpha} (V^*)_{\alpha 4} h_j \hat{I}_{\alpha k j i} \right], \qquad (16)$$

where the factor 3 is a color factor and D_d is the normalized down quark mass matrix,

$$D_d = \mathrm{diag}\left[\frac{m_d}{m_b}, \frac{m_s}{m_b}, 1 \right] . \qquad (17)$$

The function $\hat{I}_{\alpha k i j}$ is a sum of loop integrals defined as

$$\hat{I}_{\alpha k i j} = \sum_{n=1}^{3} \hat{I}^{(n)}_{\alpha k} + \sum_{n=4}^{6} \hat{I}^{(n)}_{\alpha k i} + \sum_{n=7}^{9} \hat{I}^{(n)}_{\alpha k j} , \qquad (18)$$

where the integral $\hat{I}^{(n)}$ are given by[1]

$$\begin{aligned} \hat{I}^{(1)}_{\alpha k} + \hat{I}^{(2)}_{\alpha k} &= \left(\frac{M_2^2 - M_1^2}{m_W^2} \right) \int \frac{d^4 k}{(2\pi)^4} \frac{d^4 q}{(2\pi)^4} \frac{(\not{k} + \not{q})\not{k}}{k^2} \left(1 + \xi \frac{m_W^2}{k^2 - \xi m_W^2} \right) \\ &\times \frac{1}{q^2 - M_1^2} \frac{1}{q^2 - m_{d_k}^2} \frac{1}{(k+q)^2 - M_2^2} \frac{1}{(k+q)^2 - m_{u_\alpha}^2}, \end{aligned} \qquad (19)$$

$$\begin{aligned} \hat{I}^{(3)}_{\alpha k} &= \int \frac{d^4 k}{(2\pi)^4} \frac{d^4 q}{(2\pi)^4} \frac{\not{k} + \not{q}}{k^2 - m_W^2} \left[-\not{k} - 2\not{q} + \frac{\not{k}\, k \cdot (k + 2q)}{k^2} \left(1 - \xi \frac{k^2 - m_W^2}{k^2 - \xi m_W^2} \right) \right] \\ &\times \frac{1}{q^2 - M_1^2} \frac{1}{q^2 - m_{d_k}^2} \frac{1}{(k+q)^2 - M_2^2} \frac{1}{(k+q)^2 - m_{u_\alpha}^2}, \end{aligned} \qquad (20)$$

$$\begin{aligned} \hat{I}^{(4)}_{\alpha k i} &= \int \frac{d^4 k}{(2\pi)^4} \frac{d^4 q}{(2\pi)^4} \left[4\not{k}(\not{k} + \not{q}) - (\not{k} + \not{q})\not{k} \left(1 - \xi \frac{k^2 - m_W^2}{k^2 - \xi m_W^2} \right) \right] \frac{1}{k^2 - m_W^2} \frac{1}{k^2 - m_{e_i}^2} \\ &\times \frac{1}{q^2 - M_1^2} \frac{1}{q^2 - m_{d_k}^2} \frac{1}{(k+q)^2 - m_{u_\alpha}^2}, \end{aligned} \qquad (21)$$

$$\begin{aligned} \hat{I}^{(5)}_{\alpha k i} + \hat{I}^{(6)}_{\alpha k i} &= -\left(\frac{m_{e_i}}{m_W} \right)^2 \int \frac{d^4 k}{(2\pi)^4} \frac{d^4 q}{(2\pi)^4} \frac{(\not{k} + \not{q})\not{k}}{k^2} \left(1 + \xi \frac{m_W^2}{k^2 - \xi m_W^2} \right) \frac{1}{k^2 - m_{e_i}^2} \\ &\times \frac{1}{q^2 - M_1^2} \frac{1}{q^2 - m_{d_k}^2} \frac{1}{(k+q)^2 - m_{u_\alpha}^2}, \end{aligned} \qquad (22)$$

$$\begin{aligned} \hat{I}^{(7)}_{\alpha k j} &= \int \frac{d^4 k}{(2\pi)^4} \frac{d^4 q}{(2\pi)^4} \frac{(\not{k} + \not{q})\not{k}}{k^2 - m_W^2} \left(3 - \xi \frac{k^2 - m_W^2}{k^2 - \xi m_W^2} \right) \frac{1}{k^2 - m_{e_j}^2} \\ &\times \frac{1}{q^2 - m_{d_k}^2} \frac{1}{(k+q)^2 - m_{u_\alpha}^2} \frac{1}{(k+q)^2 - M_2^2}, \end{aligned} \qquad (23)$$

$$\begin{aligned} \hat{I}^{(8)}_{\alpha k j} + \hat{I}^{(9)}_{\alpha k j} &= \left(\frac{m_{e_j}}{m_W} \right)^2 \int \frac{d^4 k}{(2\pi)^4} \frac{d^4 q}{(2\pi)^4} \frac{(\not{k} + \not{q})\not{k}}{k^2} \left(1 + \xi \frac{m_W^2}{k^2 - \xi m_W^2} \right) \frac{1}{k^2 - m_{e_j}^2} \\ &\times \frac{1}{q^2 - m_{d_k}^2} \frac{1}{(k+q)^2 - m_{u_\alpha}^2} \frac{1}{(k+q)^2 - M_2^2}. \end{aligned} \qquad (24)$$

[1]Owing to the unitarity of V, only terms containing m_{u_α} are relevant in generating neutrino mass (see Eq. (16)). All terms that are independent of m_{u_α} will add up to zero, and therefore, such terms are not written explicitly.

It is straightforward to show that all terms containing the gauge parameter ξ in Eqs. (19)-(24) add up to zero. This means that the neutrino mass matrix elements, which are physical parameters, are gauge independent. An interplay of all diagrams of Fig. 1 is required to see this gauge independence, although this can be inferred before doing the momentum integrals. Note that the contributions to these integrals proportional to charged lepton masses are strongly suppressed as can be seen from Eqs. (21)-(24). Thus, it is a good approximation to work in the limit $m_{e_i} \simeq 0$. In this limit, the neutrino mass matrix is reduced to a rank two matrix with a suppressed determinant det $(M_\nu) \ll (0.01 \text{ eV})^3$. Thus, we have a prediction that the lightest neutrino is essentially massless. For the purpose of evaluating these integrals we can also set the down quark masses to zero. Thus, the neutrino mass matrix of Eq. (16) can be written as

$$(M_\nu)_{ij} \simeq \frac{3}{2} g^2 m_b \left[h_i (V^\dagger)_{4\alpha} V_{\alpha k} (D_d)_k (g^T)_{kj} + g_{ik} (D_d)_k V_{k\alpha} V^*_{\alpha 4} h_j \right] I_\alpha, \tag{25}$$

with $I_\alpha \equiv \hat{I}_{\alpha kij}(m_{d_k} \simeq m_{e_i} \simeq m_{e_j} \simeq 0)$. The asymptotic behavior of the integral I_α (in the limit $M_1 = M_2$) is given by

$$I_\alpha = \begin{cases} \left(\frac{m_{u_\alpha}}{M_1}\right)^2 \left[-6 \ln \left(\frac{m_{u_\alpha}}{M_1}\right)^2 - \frac{\pi^2}{2} + \frac{9}{2} \right] - \pi^2 + \frac{15}{2}, \text{ for } M_1 \gg m_{u_\alpha}, m_W, \\ \frac{3}{2} \ln^2 \left(\frac{m_{u_\alpha}}{M_1}\right)^2 + \frac{\pi^2}{2} + 6, \text{ for } m_{u_\alpha} \gg M_1, \\ \left(6 - \frac{\pi^2}{4}\right) \left[\left(\frac{m_{u_\alpha}}{M_1}\right)^2 - 1 \right] - \frac{\pi^2}{2} + 9, \text{ for } m_{u_\alpha} \sim M_1 \gg m_W. \end{cases} \tag{26}$$

These expressions are very helpful, especially for analytic approximations of the integrals where the internal quarks are light quarks, and also as cross checks of the exact numerical calculations.

2.2 Neutrino mass matrix

The neutrino mass matrix of the model can now be written down:

$$M_\nu = m_0 \begin{pmatrix} x & \frac{1}{2}\frac{h_1}{h_2} y + \frac{1}{2}\frac{h_2}{h_1} x & \frac{1}{2}\frac{h_1}{h_3} + \frac{1}{2}\frac{h_3}{h_1} \\ \frac{1}{2}\frac{h_1}{h_2} y + \frac{1}{2}\frac{h_2}{h_1} x & y & \frac{1}{2}\frac{h_2}{h_3} + \frac{1}{2}\frac{h_3}{h_2} y \\ \frac{1}{2}\frac{h_1}{h_3} + \frac{1}{2}\frac{h_3}{h_1} x & \frac{1}{2}\frac{h_2}{h_3} + \frac{1}{2}\frac{h_3}{h_2} y & 1 \end{pmatrix}, \tag{27}$$

where

$$\begin{aligned} m_0 &\equiv \frac{3 g^2 m_b}{(16\pi^2)^2} h_3 F_3; \quad x \equiv \left(\frac{h_1 F_1}{h_3 F_3}\right); \quad y \equiv \left(\frac{h_2 F_2}{h_3 F_3}\right); \\ F_j &\equiv g_{jk} (V^\dagger)_{4\alpha} V_{\alpha k} (D_d)_k I_\alpha \ , \end{aligned} \tag{28}$$

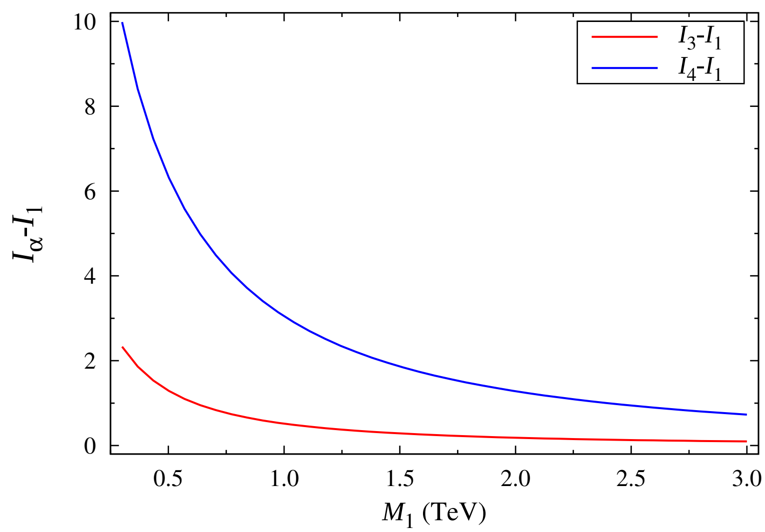

Figure 2: Plots of the integral functions $I_3 - I_1$ and $I_4 - I_1$ versus the leptoquark mass M_1. The mass of the vector-like quark is taken here to be 600 GeV, with $M_1 - M_2 = 60$ GeV.

with repeated indices assumed to be summed. By using the unitarity of the mixing matrix V, and the fact that $m_u, m_c \ll m_t, m_{t'}$ we have

$$V^*_{\alpha 4} V_{\alpha k} I_\alpha \simeq V^*_{34} V_{3k} \left(I_3 - I_1 \right) + V^*_{44} V_{4k} \left(I_4 - I_1 \right). \tag{29}$$

Plots of $I_3 - I_1$ and $I_4 - I_1$ as function of the leptoquark mass M_1 are shown in Fig. 2, for a fixed value of the vector-quark mass of 600 GeV.

To illustrate the range of parameters allowed by the neutrino mass, let us assume $g_{jk} \ll g_{j3},\ k = 1, 2$, so that only g_{j3} contribute to the neutrino mass matrix. If we further assume that only the the top quark (among u, c, t) mixes significantly with the vector-like quark, i.e., $f_1, f_2 \ll f_3$, then $V^*_{34} V_{33} \simeq -V^*_{44} V_{43} \simeq f_3 v / M$. Therefore, we can write

$$F_j \simeq \frac{g_{j3} f_3 v}{M} \left(I_3 - I_4 \right). \tag{30}$$

For normal neutrino mass hierarchy, $m_0 \simeq 0.03$ eV is needed, which in turn requires $h_3 F_3 \simeq 10^{-7}$. This means that for order one values of the Yukawa couplings h_i, f_3, g_{j3}, the mass of the vector-like quark and/or the leptoquarks is of order 10^8 GeV. Conversely, if both the LQ and vector-like quark have masses of order TeV, and if $h_3 \sim 1$, one must have $g_{33} f_3 \sim 10^{-5}$. In both regimes, lepton flavor violation processes do not strongly constrain the model parameters. Interesting new effects will arise, however, if the vector-like quark/leptoquark masses are near a TeV, and if some of the Yukawa couplings lie in the range $10^{-2} - 1$, as will be discussed in the next section.

Although the model predicts the lightest neutrino to be essentially massless, owing to the highly suppressed determinant of M_ν, Eq. (28) does admit both the normal hierarchy

(NH) and the inverted hierarchy (IH) of neutrino masses. Since the off-diagonal elements of M_ν are uniquely related to the diagonal elements, one can determine the values of h_i/h_j for $i < j$ as

$$\frac{h_i}{h_j} = \frac{(M_\nu)_{ij}}{(M_\nu)_{jj}} \left[1 \pm \sqrt{1 - \frac{(M_\nu)_{jj}(M_\nu)_{ii}}{(M_\nu)_{ij}^2}} \right], \tag{31}$$

where $(M_\nu)_{ij}$ are obtained from

$$M_\nu = U^*_{\rm PMNS}(M_\nu)_{\rm diag} U^\dagger_{\rm PMNS}. \tag{32}$$

Here $U_{\rm PMNS}$ is the leptonic mixing matrix parameterized as in Ref. [21], while $(M_\nu)_{\rm diag}$ is given by

$$\begin{aligned} (M_\nu)_{\rm diag} &= {\rm diag}\ \left(0, m_2 e^{i\alpha}, m_3\right), \text{ for NH}, \\ (M_\nu)_{\rm diag} &= {\rm diag}\ \left(m_1, m_2 e^{i\alpha}, 0\right), \text{ for IH}. \end{aligned} \tag{33}$$

Take for example the ratio h_2/h_3. Its value can be determined from Eq. (31), but this must match the product $(h_2/h_1)(h_1/h_3)$, also obtained from the same equation. Now, by using the central values of the current neutrino oscillation data, $\Delta m^2_{\rm sol} = 7.59 \times 10^{-5}$ eV^2, $\Delta m^2_{\rm atm} = 2.3 \times 10^{-3}$ eV^2, $\sin^2\theta_{12} = 0.304$, $\sin^2\theta_{23} = 0.5$, and the upper limit on θ_{13}, $\sin^2\theta_{13} \leq 0.04$ [22], one can find the allowed values of h_2/h_3. This result is plotted in Fig. 3 versus $\sin^2\theta_{13}$, both for NH (upper left panel) and for IH (upper right panel). From this figure we see that the ratio of h_2/h_3 has to be of order one for normal hierarchy, while it can range from 0.5 to 1000 for inverted hierarchy. In both cases the value of θ_{13} is allowed to range from zero up to the current upper limit. Recently the T2K experiment [23] has reported an indication of nonzero θ_{13}, with the best fit value (assuming $\sin^2 2\theta_{23} = 1$ and $\delta = 0$) being $\sin^2 2\theta_{13} = 0.11$ (0.14) for normal (inverted) hierarchy. MINOS experiment also finds supporting evidence, although with less significance [24]. The present model can accommodate these indications for a sizable θ_{13}.

The couplings h_i will mediate $\ell_i \to \ell_j\gamma$ decays (see the next section for detailed discussions). One has for the ratio of branching ratios,

$$\frac{{\rm BR}\ (\mu \to e\gamma)}{{\rm BR}\ (\tau \to e\gamma)} = \left|\frac{h_2}{h_3}\right|^2 \times {\rm BR}(\tau \to e\overline{\nu}_e\nu_\tau), \tag{34}$$

where ${\rm BR}(\tau \to e\overline{\nu}_e\nu_\tau) \simeq 0.18$ [21]. Eq. (34) has an interesting consequence. As explained above, in the NH case, $|h_2/h_3| \sim 1$. This means the branching ratio of $\tau \to e\gamma$ cannot exceed 5.3×10^{-11} because of the limit on the branching ratio ${\rm BR}(\mu \to e\gamma) < 2.4 \times 10^{-12}$ [25]. A measurement of BR $(\tau \to e\gamma)$ near the current experimental limit of $\sim 10^{-8}$ would rule out the NH scenario. Of course, for these decays to have significant branching ratios, the leptoquarks must have masses not much above a TeV. In Fig. 3, we also show the ratio

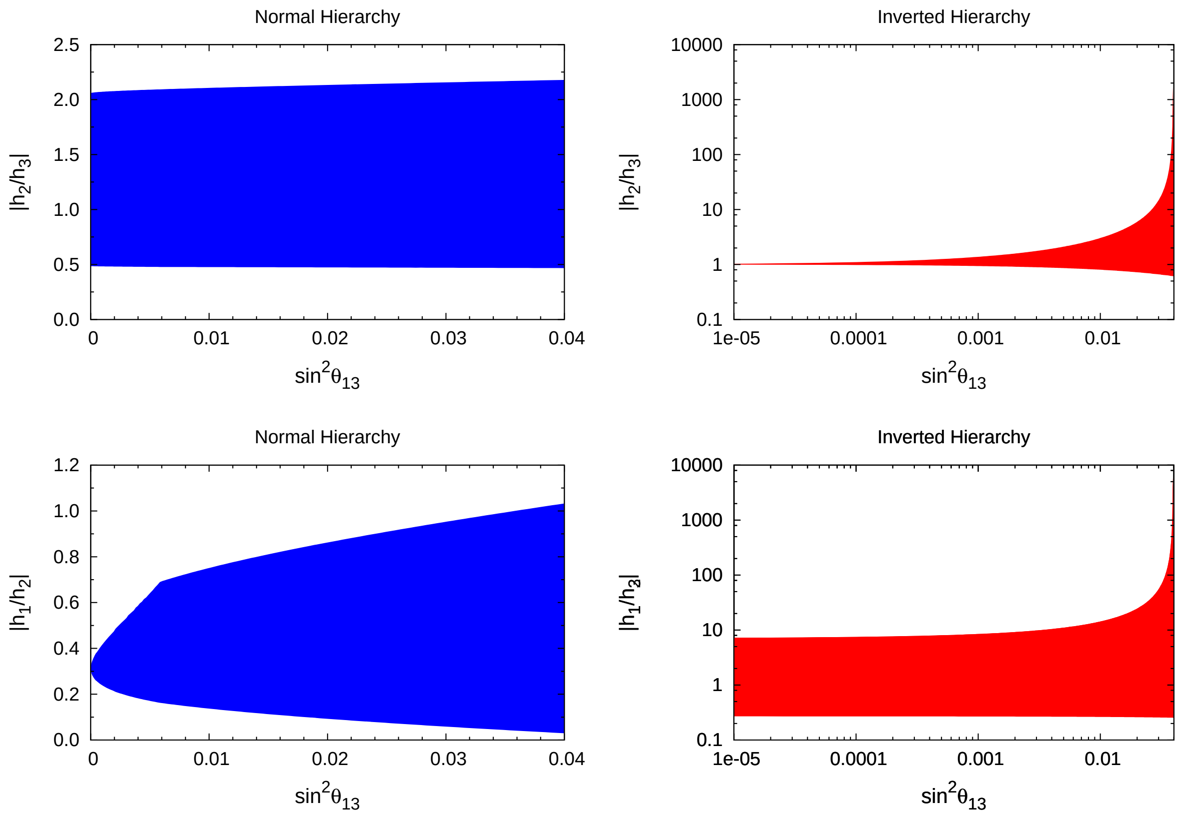

Figure 3: Plots of the allowed values of h_i/h_j as a function of $\sin^2\theta_{13}$ for normal hierarchy (left panel) and inverted hierarchy (right panel).

$|h_1/h_2|$ as a function of $\sin^2\theta_{13}$ allowed in the model for the NH case (lower left panel) and IH case (lower right panel). The ratio $\mathrm{BR}(\tau \to e\gamma)/\mathrm{BR}(\tau \to \mu\gamma) = |h_1/h_2|^2$ can serve as a further test of our model.

3 Experimental constraints

The new interactions shown in Eqs. (5) and (15) can induce lepton flavor violation processes such as $\mu \to e\gamma$ and $\mu \to 3e$ decays. In this section we analyze various such processes and derive limits on model parameters. LHC experiments have set lower limits on the leptoquark mass: $M_{1,2} > 376\,(319)$ GeV for the first generation leptoquarks and $M_{1,2} > 422\,(362)$ GeV for the second generation leptoquarks, assuming branching ratio of 1(0.5) [26]. Our fit to neutrino mass suggests that the branching ratio of the leptoquark to muons is about 0.5, so we shall adopt the corresponding limits in this section. Recent results from the CMS collaboration at LHC has set a limit $m_{t'} > 475$ GeV for a vector-like iso-singlet quark mass, assuming that t' decays to tZ with 100% branching ratio [27]. We choose mass values consistent with this constraint, with a nominal value of $m_{t'} = 600$ GeV.

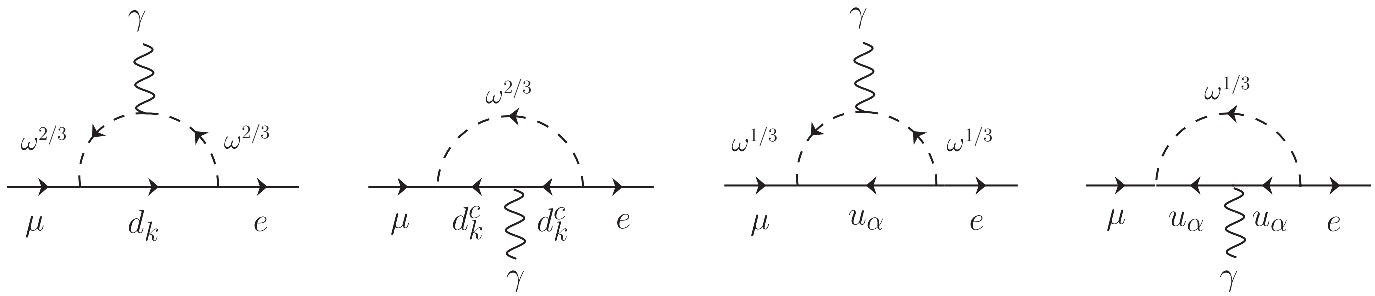

Figure 4: One loop diagrams leading to $\mu \to e\gamma$ decay.

3.1 $\mu \to e\gamma$

This process occurs in the model via the one loop diagrams shown in Fig. 4. There are two couplings which are responsible for this process: g_{ij} and h_i. In fact, the predictions of this model are similar to the ones discussed in Ref. [12], with one difference that here we have interference between diagrams generated by g_{ij} and those induced by h_i. In the present model, ignoring the electron mass, which is an excellent approximation, the branching ratio is given by

$$\mathrm{BR}(\mu \to e\gamma) = \frac{27\alpha}{16\pi G_F^2} \left| F(x_{d_i}) \frac{g_{1i}^* g_{2i}}{M_2^2} + H(x_{u_\alpha}) V_{\alpha 4}^* V_{\alpha 4} \frac{h_1^* h_2}{M_1^2} \right|^2 , \tag{35}$$

where $x_{d_i} \equiv m_{d_i}^2/M_2^2$ and $x_{u_\alpha} \equiv m_{u_\alpha}^2/M_1^2$. The dimensionless functions $F(x)$ and $H(x)$ are given by [28, 29]

$$\begin{aligned} F(x) &= -\frac{x}{12} \frac{(1-x)(5+x) + 2(2\,x+1)\ln x}{(1-x)^4}, \\ H(x) &= -\frac{1}{12} \frac{(1-x)(5\,x+1) + 2\,x(2+x)\ln x}{(1-x)^4}. \end{aligned} \tag{36}$$

The branching ratios for other $\ell_i \to \ell_j\gamma$ processes can be derived in a similar way. The resulting constraints on the model parameters are summarized in Table 1. Here all of the experimental limits are taken from Ref. [21] except for $\mu \to e\gamma$ limit which is taken from Ref. [25].

An interesting feature of this analysis is that the g_{ij} couplings are only weakly constrained from these processes. This is owing to a GIM–like cancelation for the amplitude for this process from the first two diagrams of Fig. 4. This is similar to the model discussed in Ref. [12]. This cancelation occurs, in the limit of down quark mass being zero, since the charge of the internal leptoquark (2/3) is twice as large and opposite in sign compared to the charge of of the internal down quark ($-1/3$). The amplitude for the diagram when the photon is emitted from the scalar line is twice smaller compared to the diagram where it is emitted from the fermion line, which leads to the cancelation. The amplitude that survives has a suppression of (m_b^2/M_2^2), which causes the weak limit. Because of this cancelation,

Process	BR limit	Constraint
$\mu \to e\gamma$	$< 2.4 \times 10^{-12}$	$\left\| F(x_{d_i})\frac{g_{1i}^* g_{2i}}{M_2^2} + H(x_{u_\alpha})V_{\alpha 4}^* V_{\alpha 4}\frac{h_1^* h_2}{M_1^2}\right\|^2 < \frac{1.39\times 10^{-19}}{\text{GeV}^4}$
$\tau \to e\gamma$	$< 3.3 \times 10^{-8}$	$\left\| F(x_{d_i})\frac{g_{1i}^* g_{3i}}{M_2^2} + H(x_{u_\alpha})V_{\alpha 4}^* V_{\alpha 4}\frac{h_1^* h_3}{M_1^2}\right\|^2 < \frac{4.8\times 10^{-5}}{\text{GeV}^4}$
$\tau \to \mu\gamma$	$< 4.4 \times 10^{-8}$	$\left\| F(x_{d_i})\frac{g_{2i}^* g_{3i}}{M_2^2} + H(x_{u_\alpha})V_{\alpha 4}^* V_{\alpha 4}\frac{h_2^* h_3}{M_1^2}\right\|^2 < \frac{6.6\times 10^{-15}}{\text{GeV}^4}$

Table 1: Constraints on model parameters from $\ell_i \to \ell_j\gamma$.

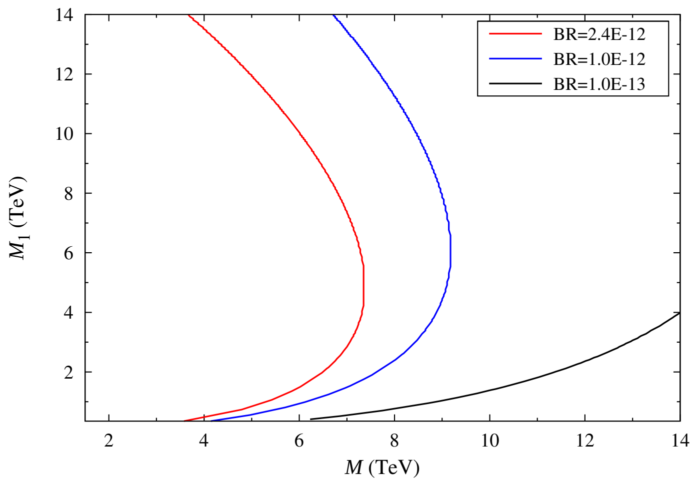

Figure 5: The allowed region for for the leptoquark mass M_1 versus the vector-like quark mass M from $\mu \to e\gamma$. Here regions left of a contour is allowed for a fixed value of the branching ratio. Thus, if $\text{BR}(\mu \to e\gamma) = 1.0 \times 10^{-12}$ is measured, the masses must lie to the left of the blue contour.

we can derive correlated limits on the masses of the leptoquarks and the vector-like quark from $\mu \to e\gamma$, since only the h_i couplings are involved. This is shown as a contour plot in Fig. 5. To get the largest possible masses, we set the Yukawa couplings $h_1 = h_2 = 1$, as large as allowed by perturbativity. If $\mu \to e\gamma$ is discovered at the current limit [25] the masses should lie to the left of the red contour in Fig. 5, while a measurement of $\text{BR}(\mu \to e\gamma) = 1.0 \times 10^{-12}$ would require the masses to lie to the left of the blue contour. The LHC reach for a leptoquark of this type is 1.5 TeV [30], which would serve as a cross check in this case.

3.2 $\mu \to 3e$

In this process, the photon can be off-shell, and therefore, there is no GIM-like cancelation for the g_{ij} contributions. It turns out that in addition to the photon penguin diagrams, there are also Z penguin diagrams and box diagrams (the Higgs boson exchange is suppressed by the electron mass). The mixing between vector-like quark and SM chiral quarks also plays a role in this process. The expression for the decay width is rather lengthy, which we do not present for brevity, but it is similar to the one given in Ref. [12]. To simplify the problem in deriving the constraints, we assume that only the top quark mixes with the vector-like quark, or equivalently $s_{14}, s_{24} \ll \lambda^3$ in Eq. (14), where $\lambda \simeq 0.22$ is the Wolfenstein parameter, while s_{34} could be as large as 0.3, consistent with constraint from $Z \to b\bar{b}$ constraint [31]. For $\omega^{2/3}$ exchange (corresponding to down-type quark inside the loop), we assume that there is no accidental cancelation among the different couplings g_{ij}, and thus omit terms such as $g_{13}g_{23}g_{jk}$ with $j, k = 1, 2$. For degenerate leptoquark masses of 400 GeV, and for the vector-like quark mass set equal to 600 GeV, we obtain:

$$|h_1 h_2| < 2.7 \times 10^{-4}(3.4 \times 10^{-4}); \; |g_{13}g_{23}| < 1.7 \times 10^{-3}; \; |g_{1j}g_{2j}| < 8.6 \times 10^{-4}, \; j = 1, 2, \quad (37)$$

for $c_{34} = 0.98\,(1.0)$. These limits are obtained by assuming that contributions from one type of coupling dominates at a time. While these limits are stringent, they do not pose any restriction on the neutrino masses and mixings. The decay $\mu \to 3e$ may be within reach of next generation experiments, with the couplings lying in the range $(10^{-2} - 1)$ and the leptoquark mass around a TeV.

3.3 $\mu - e$ conversion in nuclei

Since this model features direct interactions of quark and lepton via the leptoquarks, $\mu - e$ conversion in nuclei occurs. The diagrams are similar to the ones discussed in Ref. [12], with tree level and loop contributions. There is a more direct link between neutrino mass and the loop induce $\mu - e$ conversion process. If we assume that only the top quark mixes with the vector-like quark as in the case of $\mu \to 3e$, then there is no tree level $\omega^{-1/3}$ exchange contribution to this process. Following the procedure outlined in Ref. [12], from the limit on $\mu - e$ conversion in ^{48}Ti, we obtain (for $M_{LQ} = 400$ GeV, and a vector-like quark mass of 600 GeV)

$$|h_1 h_2| < 2.2 \times 10^{-4}(9.8 \times 10^{-3}); \; |g_{13}g_{23}| < 8.7 \times 10^{-4}; \; |g_{11}g_{21}| < 4.6 \times 10^{-6}, \quad (38)$$

for $c_{34} = 0.95\,(1.0)$. Again, this analysis suggests that for natural values of the model parameters, this process may be within reach of next generation experiments.

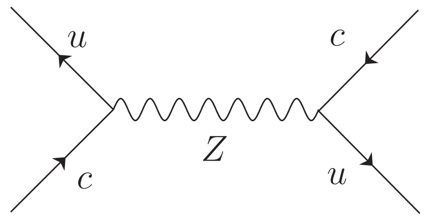

Figure 6: Tree level Z exchange diagram leading to $D^0 - \overline{D^0}$ mixing.

3.4 Tree level $D^0 - \overline{D^0}$ mixing

The FCNC that occurs in the up–quark sector (see Eq. (12)) induces tree level $D^0 - \overline{D^0}$ mixing mediated by the Z boson, as shown in Fig. 6. The neutral Higgs boson induced contribution from Eq. (13) is suppressed by light quark mass and can be ignored. The mixing amplitude is given by [32]

$$M_{12}^{\rm new} = \frac{\sqrt{2}G_F}{3}\ (V_{14}V_{24}^*)^2\ m_D f_D^2 \hat{B}_D \eta_D(\mu), \tag{39}$$

where $m_D = 1.9$ GeV is the D meson mass, $f_D = 0.201$ GeV is the D meson decay constant, $\hat{B}_D(\mu \sim m_D) = 0.865$ is the bag parameter, and $\eta_D(\mu \sim m_D) = 0.78$ is the QCD correction factor. All the numbers here are taken from Ref. [33]. By using $\Delta m_D = 1.6 \times 10^{-14}$ GeV [21], one obtains the constraint

$$|V_{14}V_{24}^*| < 2.5 \times 10^{-4}. \tag{40}$$

According to Eq. (14) this constraint implies $|c_{14}s_{14}s_{24}| < 2.5 \times 10^{-4}$. As a result of this limit, unlike in a four generation model where there is no such FCNC process, the vector–quark contributions to meson mixing (eg., in the B_d^0 sector) cannot be too large.

3.5 $B_s^0 \to \mu^+\mu^-$ decay

Recently the CDF collaboration has reported a hint for the decay $B_s^0 \to \mu^+\mu^-$, with $\mathrm{BR} = \left(1.8^{+1.1}_{-0.9}\right) \times 10^{-8}$ [34]. LHCb collaboration has not confirmed such a hint, and quotes an upper limit $\mathrm{BR}(B_s^0 \to \mu^+\mu^-) < 1.4 \times 10^{-8}$ [35]. The SM prediction for this branching ratio is $\mathrm{BR}(B_s^0 \to \mu^+\mu^-) = 3.2 \times 10^{-9}$, which means there is ample room for new physics in this process.

Tree level exchange of leptoquarks can contribute to $B_s^0 \to \mu^+\mu^-$ decay in our model. The branching fraction is given by [36]

$$\mathrm{BR}(B_s^0 \to \mu^+\mu^-) = \frac{|g_{22}g_{23}|^2}{128\pi M_2^4}\tau_{B_s} f_{B_s}^2 m_{B_s} m_\mu^2 \sqrt{1 - 4\frac{m_\mu^2}{M_2^2}} \tag{41}$$

where the SM contributions have been ignored. This enables us to fit $\mathrm{BR}(B_s^0 \to \mu^+\mu^-) = 1.8 \times 10^{-8}$, with $M_2 = 400$ GeV for the leptoquark mass, and $|g_{22}g_{23}| \sim 4.2 \times 10^{-3}$.

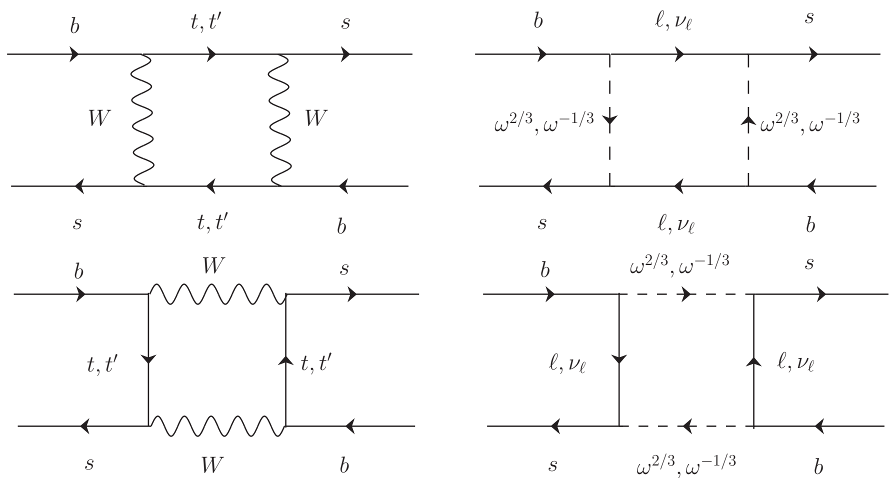

Figure 7: Box diagrams leading to $B_s^0 - \overline{B_s^0}$ mixing.

3.6 New CP violation in $B_s^0 - \overline{B_s^0}$ mixing

Our model of leptoquarks and vector-like quark generates new contributions to $B_s^0 - \overline{B_s^0}$ mixing. There are two sources, one through LQ induced box diagrams, and the other through SM-like box diagrams with the vector-like quark (see Fig. 7). Including these contributions, the $B_s^0 - \overline{B_s^0}$ mixing amplitude becomes

$$\begin{aligned} M_{12s} \;=\; & \left\{ \frac{G_F^2 m_W^2}{12\pi^2} \left[(V_{32}^* V_{33})^2 \eta_{33} S_0(x_3) + 2\,(V_{32}^* V_{33})\,(V_{42}^* V_{43})\,\eta_{34} S_0(x_3, x_4) + (V_{42}^* V_{43})^2 \eta_{44} S_0(x_4) \right] \right. \\ & \left. + \frac{(g_{i2} g_{i3}^*)^2}{192\pi^2 M_2^2} \eta_B \right\} m_{B_s} f_{B_s}^2 \hat{B}_s(\mu). \end{aligned} \tag{42}$$

The functions $S_0(x_\alpha), S_0(x_\alpha, x_\beta)$ with $x_\alpha \equiv m_{u_\alpha}^2/m_W^2$ are the Inami-Lim functions [37], whereas η_{ij}, η_B with $i, j = 3, 4$ are the QCD correction factors. The numerical values for these factors for a 600 GeV vector-like quark mass are [38]

$$\eta_{33} = \eta_B = 0.5765,\ \eta_{34} = \eta_{44} = 0.514. \tag{43}$$

It is sometimes more convenient to parameterize M_{12s} as [39]

$$\frac{M_{12s} - M_{12s}^{\rm SM}}{M_{12s}^{\rm SM}} \;\equiv\; r_{1s} e^{i2\sigma_{1s}} + r_{2s} e^{i2\sigma_{2s}} \tag{44}$$

where $\{r_{1s}, \sigma_{1s}\}$ and $\{r_{2s}, \sigma_{2s}\}$ are the new contributions coming from vector–like quark mixing and LQ box diagrams respectively. With this parameterization, one can write,

$$\begin{aligned} \Delta m_{B_s} &= \Delta m_{B_s}^{\rm SM} \left| 1 + r_{1s} e^{i2\sigma_{1s}} + r_{2s} e^{i2\sigma_{2s}} \right|, \\ S_{J/\psi\phi} &= \sin\left[2\beta_s^{\rm SM} - {\rm Arg}\left(1 + r_{1s} e^{i2\sigma_{1s}} + r_{2s} e^{i2\sigma_{2s}} \right) \right], \end{aligned} \tag{45}$$

with $\beta_s^{\rm SM} \equiv {\rm Arg}\left[(-V_{32} V_{33}^*) \,/\, (V_{22} V_{23}^*) \right] = 0.019 \pm 0.001$ and $\Delta m_{B_s}^{\rm SM} = (19.3 \pm 6.74)$ ps^{-1} [40].

The main reason to highlight this phenomenon is that there appears to be hints for new physics in CP violation in the B system. The DØ collaboration has reported a measurement of the charge asymmetry in the same sign di-muon decay of the B mesons [16]:

$$A_{sl}^b = \frac{N^{++} - N^{--}}{N^{++} + N^{--}} = -(0.787 \pm 0.172 \pm 0.093)\%. \qquad (46)$$

Here $N^{++}(N^{--})$ is the number of events containing two b hadrons that decay semileptonically into two positive (negative) muons. Eq. (46) can be written as a linear combination of two asymmetries [16, 41]

$$A_{sl}^b = (0.506 \pm 0.043) a_{sl}^d + (0.494 \pm 0.043) a_{sl}^s, \qquad (47)$$

where a_{sl}^q $(q \equiv d, s)$ is defined as [16]

$$a_{sl}^q = \frac{\Gamma(\overline{B}_q \to \mu^+ X) - \Gamma(B_q \to \mu^- X)}{\Gamma(\overline{B}_q \to \mu^+ X) + \Gamma(B_q \to \mu^- X)}. \qquad (48)$$

In the SM, $a_{sl}^d = -4.8^{+1.0}_{-1.2} \times 10^{-4}$ and $a_{sl}^s = (2.1 \pm 0.6) \times 10^{-5}$ [40], so that $(A_{sl}^b)^{\rm SM} = -2.3^{+0.5}_{-0.6} \times 10^{-4}$ which is 3.9σ away from the DØ measurement (see Eq. (46)). A likely explanation is that there is a new source of CP violation in $B_s^0 - \overline{B_s^0}$ mixing.

Additionally, the measurements of relative phase between B_s^0 mixing amplitude and $B_s^0 \to J/\psi\phi$ decay amplitude ($S_{J/\psi\phi} \equiv \sin 2\beta_s^{J/\psi\phi}$) performed by CDF [42] and DØ [43] yield [44]:

$$\beta_s^{J/\psi\phi} \;=\; 0.47^{+0.13}_{-0.21} \;\cup\; 1.09^{+0.21}_{-0.13}, \qquad (49)$$

Here there is a 2.1σ discrepancy from SM prediction for β_s, which may be another hint for physics beyond the SM, although not very significant.

It is interesting to see whether the vector–like charge 2/3 quark can resolve these problems. The best fit to the data for a fourth generation quarks, including the preferred values of the CKM mixing angles, is given in Ref. [47] which quotes $\beta_s = 0.03$, corresponding to $r_{1s} = 0.02$. This value is quite far from the experimental central value (see Eq. (49)). This result should be applicable in the present model as well. We conclude that the mixing with vector-like quark is not enough to get the central value of β_s, so the LQ induced box diagram is a more promising source for the new physics here.

Ignoring the effect of extra family mixing, the LQ contribution $\{r_{2s}, \sigma_{2s}\}$, can satisfy the best fit given in Ref. [39], i.e. $\{0.5, 120°\}$. This would correspond to $|g_{i2}g_{i3}| \sim 0.06$ with $M_2 = 400$ GeV, where the index i is summed. However, since the limits $\text{BR}(B_s^0 \to \mu^+\mu^-) < 10^{-8}$ and $\text{BR}(B_s^0 \to e^+e^-) < 2.8 \times 10^{-7}$ must be satisfied, the dominant contribution should arise with the τ and ν_τ inside the leptoquark box diagram. The phase is not constrained and therefore can take the fitted value of 120°.

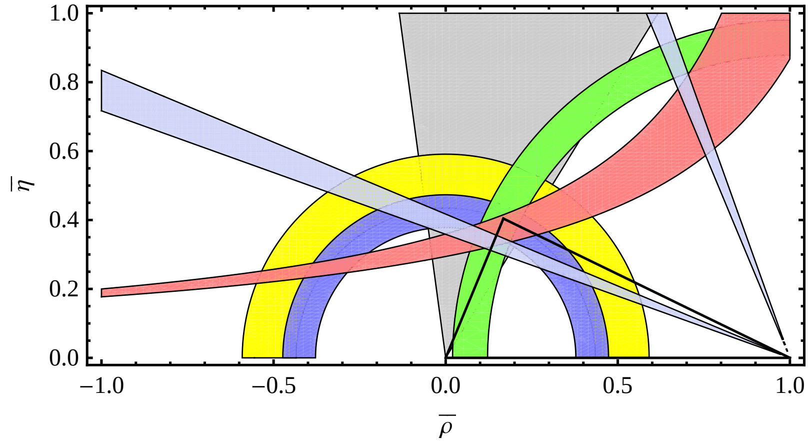

Figure 8: The unitarity triangle fit leading to $\sin 2\beta$ determination.

3.7 $\sin 2\beta$ versus ϵ_K

Analogous to the B_s^0 system, this model also provides new contributions to $B_d^0 - \overline{B_d^0}$ mixing, arising through LQ induced box diagrams and new mixing between SM quarks and the vector-like quark. Owing to the stringent constraint arising from the tree level $D^0 - \overline{D^0}$ mixing, see Eq. (40), analogous mixing in the K^0 system would be more suppressed. Currently, there is a 2.5σ tension in $\sin 2\beta$ determination obtained from $B_d^0 \to J/\psi K_S$ which gives [44]

$$S_{J/\psi K_S} = \sin 2\beta^{\rm exp} = 0.673 \pm 0.023, \tag{50}$$

and the one inferred from unitarity triangle fit with three generations of SM [45]

$$\sin 2\beta^{\rm fit} = 0.761 \pm 0.034. \tag{51}$$

Note that this fit strongly depends on the input value of $|V_{ub}|$. The authors of Ref. [17] opt to drop $|V_{ub}|$ gotten from exclusive and/or inclusive measurements due to the large disparity between the two. Instead, they use $|V_{ub}|$ obtained from ${\rm BR}(B^- \to \tau^- \nu)$. This causes $\sin 2\beta^{\rm fit}$ to shift to a larger value compared to the one shown in Eq. (51), and thus increases the tension with the direct measurement of $S_{J/\psi K_S}$. (The fit quoted in Eq. (51) does not include $|V_{ub}|$ obtained from ${\rm BR}(B^- \to \tau^- \nu)$.) For detailed discussions and assumptions, see [17, 45].

Here we present a fit to $\sin 2\beta$ by using $|V_{ub}|$ obtained from both direct measurements and ${\rm BR}(B^- \to \tau^- \nu)$. The numerical values used for this fit are: $|\epsilon_K| = (2.229 \pm 0.010) \times 10^{-3}$, $|V_{ub}| = (3.94 \pm 0.26) \times 10^{-3}$ (a global average from inclusive and exclusive decays, not including ${\rm BR}(B^- \to \tau^- \nu)$), $|V_{cb}| = (40.8 \pm 0.5) \times 10^{-3}$, ${\rm BR}(B^- \to \tau^- \nu) = (1.72 \pm 0.28) \times 10^{-4}$, $\gamma = (73 \pm 11)^\circ$ [45], and mass differences $\Delta m_{B_d} = (0.507 \pm 0.005)$ ps^{-1} and $\Delta m_{B_s} = (17.77 \pm 0.12)$ ps^{-1} [21]. Following the method given in Ref. [46], we found $\sin 2\beta^{\rm fit} = 0.79$, which is about 3σ away from the experimental value of $S_{J/\psi K_S}$. This best fit is shown as the triangle apex in Fig. 8. We can also see that this best fit lies outside the allowed region of $S_{J/\psi K_S}$ indicated by the light blue bands. A possible explanation is that there is new physics that affects the B_d^0 system, which we parameterize as

$$\frac{M_{12d} - M_{12d}^{\rm SM}}{M_{12d}^{\rm SM}} \equiv r_{1d} e^{i2\sigma_{1d}} + r_{2d} e^{i2\sigma_{2d}}, \tag{52}$$

where

$$M_{12d} = \left\{ \frac{G_F^2 m_W^2}{12\pi^2} \left[\left(V_{31}^* V_{33}\right)^2 \eta_{33} S_0(x_3) + 2 \left(V_{31}^* V_{33}\right) \left(V_{41}^* V_{43}\right) \eta_{34} S_0(x_3, x_4) + \left(V_{41}^* V_{43}\right)^2 \eta_{44} S_0(x_4) \right] + \frac{\left(g_{i1} g_{i3}^*\right)^2}{192\pi^2 M_2^2} \eta_B \right\} m_{B_d} f_{B_d}^2 \hat{B}_d(\mu). \tag{53}$$

This is analogous to the discussion of B_s^0 mixing. With this formula, one can write

$$S_{J/\psi K_S} = \sin\left[2\beta^{\rm fit} + \phi^{B_d}\right], \tag{54}$$

where

$$\phi^{B_d} = {\rm Arg}\left[1 + r_{1d} e^{i2\sigma_{1d}} + r_{2d} e^{i2\sigma_{2d}}\right]. \tag{55}$$

Unlike in the B_s^0 system, the effect of the vector-like quark can be significant and help resolve the tension in $\sin 2\beta$ determination. In order to see this effect, let us ignore for the moment the LQ contributions. Then, if we choose [47]

$$\begin{aligned} V_{31}^* V_{33} &= 0.009 e^{i0.5}, \\ V_{41}^* V_{43} &= 0.0006 e^{-i0.2}, \end{aligned} \tag{56}$$

we obtain $S_{J/\psi K_S} = 0.68$, which is in the good agreement with the experimental value. Note that the leptoquarks can also contribute to $K^0 - \overline{K^0}$ mixing and $B_d^0 - \overline{B_d^0}$ mixing. Such contributions are not strongly constrained by neutrino mass nor lepton flavor violation, so they alone can bring $\sin 2\beta$ close to the experimental value. This would require that the leptoquarks have masses less than about 500 GeV.

3.8 Neutrinoless double beta decay

Our model can accommodate the inverted neutrino mass hierarchy in which case neutrinoless double beta decay ($\beta\beta_{0\nu}$) may be within reach of proposed experiments. Interestingly, it can also occur at an observable rate in the case of normal mass hierarchy, through the vector-scalar exchange mechanism [19], depicted in Fig. 9.

The effective Lagrangian of the new $\nu - e^c - u - d$ vertex arising from Fig. 9, after Fierz rearrangement, is

$$\mathcal{L}_{\rm eff}^{\rm new} = \frac{G_F}{\sqrt{2}} \left[\epsilon_{S+P}\, \overline{u} \left(1+\gamma_5\right) d\, \overline{\nu}_e \left(1+\gamma_5\right) e^c \; + \; \epsilon_T\, \overline{u} \sigma^{\mu\nu} \left(1+\gamma_5\right) d\, \overline{\nu}_e \sigma_{\mu\nu} \left(1+\gamma_5\right) e^c\right] \tag{57}$$

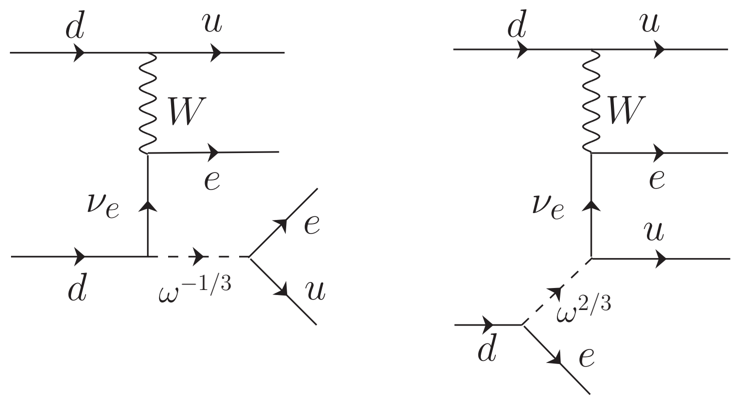

Figure 9: Diagrams leading to neutrinoless double beta decay through vector-scalar exchange.

where

$$\epsilon_{S+P} = \frac{g_{11}^* h_i V_{14}^*}{4\sqrt{2} M_1^2 G_F}\left(1 - \frac{M_1^2}{M_2^2}\right); \qquad \epsilon_T = \frac{g_{11}^* h_i V_{14}^*}{8\sqrt{2} M_1^2 G_F}\left(1 + \frac{M_1^2}{M_2^2}\right). \tag{58}$$

This process is similar to MSSM models without R-parity discussed in Ref. [19] and [48]. Following Ref. [48, 49], and by using the results from the Heidelberg-Moscow experiment on $\beta\beta_{0\nu}$ decay rate [50], one obtains for $M_1 = M_2 = 400$ GeV,

$$|g_{11}^* h_1 V_{14}^*| \leq 1.78 \times 10^{-8} \left(\frac{M_1}{400 \text{ GeV}}\right)^2. \tag{59}$$

The product of the mixing matrix elements $|V_{14}V_{24}|$ is constrained by $D^0 - \overline{D^0}$ mixing and has to be less than 2.5×10^{-4} (see Eq. (40)), which can however be satisfied by choosing $|V_{24}|$ to be small. Separately $|V_{14}| < 0.03$ is required at the 95% CL from the observed unitarity of the first row of the CKM matrix [21]. Since the coupling g_{11} is not constrained by neutrino mass, it could be of order one. For example, with $|V_{14}| \lesssim 10^{-5}$ and $h_1 \sim 10^{-2}$ and leptoquark mass of order TeV, which are all consistent with lepton flavor violation constraints, one sees that neutrinoless double beta decay can occur at an observable rate even in the case of normal mass hierarchy.

4 Conclusions

In this paper we have presented a new two-loop neutrino mass generation model which has the effective operator $\mathcal{O}_3$ of Eq. (2). Neutrino masses are naturally small, since they arise at two–loop level. The simplest way of generating this effective operator in a renormalizable theory is by the addition of a charge 2/3 vector-like quark and a scalar leptoquark doublet to the standard model spectrum. We have studied the phenomenology of the resulting model. The model admits both normal and inverted hierarchy of neutrino masses, and predicts that one of the neutrinos is essentially massless. A variety of flavor violating processes both in the lepton sector and in the quark sector are predicted. We have analyzed the correlations between such processes implied by neutrino oscillation data.

The vector–like quark and the leptoquarks of the model can explain some of the apparent anomalies that have been reported recently. There are new contributions to CP violation in the B_s^0 and in the B_d^0 system. The leptoquark–induced CP violation in $B_s^0 - \overline{B_s^0}$ mixing can explain the di-muon anomaly reported by the DØ collaboration in B hadron decays. The apparent tension in the determinations of $\sin 2\beta$ from B_d^0 decays and from the global analysis including ϵ_K from the K meson system also finds a natural explanation in this model. Neutrinoless double beta decay may occur through vector-scalar exchange and may be observable even with a normal hierarchy in the neutrino masses.

Acknowledgement

This work is supported in part by the US Department of Energy, Grant Number DE-FG02-04ER41306.

References

[1] S. Weinberg, Phys. Rev. Lett. **43**, 1566 (1979).

[2] P. Minkowski, Phys. Lett. B **67**, 421 (1977); M. Gell-Mann, P. Ramond, and R. Slansky, in *Supergravity*, eds. D. Freedman *et al.*, (North-Holland, Amsterdam, 1980); T. Yanagida, in *Proceedings of the Workshop on Baryon Number in the Universe*, eds. O. Sawada and A. Sugamoto, (KEK, 1979); R. N. Mohapatra and G. Senjanović, Phys. Rev. Lett. **44**, 912 (1980).

[3] A. Zee, Phys. Lett. B **93**, 389 (1980).

[4] T. P. Cheng and L. -F. Li, Phys. Rev. D **22**, 2860 (1980).

[5] L. J. Hall and M. Suzuki, Nucl. Phys. B **231**, 419 (1984).

[6] A. Zee, Nucl. Phys. B **264**, 99 (1986).

[7] K. S. Babu, Phys. Lett. B **203**, 132 (1988).

[8] K. S. Babu and C. N. Leung, Nucl. Phys. B **619**, 667 (2001).

[9] L. Wolfenstein, Nucl. Phys. B **175**, 93 (1980).

[10] Y. Koide, Phys. Rev. D **64**, 077301 (2001); P. H. Frampton, M. C. Oh, and T. Yoshikawa, Phys. Rev. D **65**, 073014 (2002); X. G. He, Eur. Phys. J. C **34**, 371 (2004).

[11] K. S. Babu and C. Macesanu, Phys. Rev. D **67**, 073010 (2003); M. Nebot, J. F. Oliver, D. Palao, and A. Santamaria, Phys. Rev. D **77**, 093013 (2008); D. Aristizabal Sierra and M. Hirsch, JHEP **0612**, 052 (2006).

[12] K. S. Babu and J. Julio, Nucl. Phys. B **841**, 130 (2010).

[13] K. Choi, K. S. Jeong, and W. Y. Song, Phys. Rev. D **66**, 093007 (2002).

[14] A. de Gouvea and J. Jenkins, Phys. Rev. D **77**, 013008 (2008).

[15] For a recent analysis see: P. Dey, A. Kundu, B. Mukhopadhyaya, and S. Nandi, JHEP **0812**, 100 (2008).

[16] V. M. Abazov *et al.* [D0 Collaboration], Phys. Rev. D **84**, 052007 (2011); V. M. Abazov *et al.* [D0 Collaboration], Phys. Rev. D **82**, 032001 (2010).

[17] E. Lunghi and A. Soni, Phys. Lett. B **697**, 323 (2011); E. Lunghi and A. Soni, Phys. Lett. B **666**, 162 (2008); E. Lunghi and A. Soni, arXiv:1104.2117 [hep-ph].

[18] D. Guadagnoli, arXiv:1102.2760 [hep-ph].

[19] K. S. Babu and R. N. Mohapatra, Phys. Rev. Lett. **75**, 2276 (1995).

[20] H. Harari and M. Leurer, Phys. Lett. B **181**, 123 (1986); H. Fritzsch and J. Plankl, Phys. Rev. D **35**, 1732 (1987).

[21] K. Nakamura *et al.* [Particle Data Group], J. Phys. G **37**, 075021 (2010).

[22] T. Schwetz, M. A. Tortola, and J. W. F. Valle, New J. Phys. **10**, 113011 (2008); M. Mezzetto and T. Schwetz, J. Phys. G **37**, 103001 (2010).

[23] K. Abe *et al.* [T2K Collaboration], Phys. Rev. Lett. **107**, 041801 (2011).

[24] P. Adamson *et al.* [MINOS Collaboration], Phys. Rev. Lett. **107**, 181802 (2011).

[25] J. Adam *et al.* [MEG Collaboration], Phys. Rev. Lett. **107**, 171801 (2011).

[26] G. Aad *et al.* [ATLAS Collaboration], Phys. Rev. D **83**, 112006 (2011).

[27] S. Chatrchyan *et al.* [CMS Collaboration], Phys. Rev. Lett. **107**, 271802 (2011).

[28] J. Hisano, T. Moroi, K. Tobe, and M. Yamaguchi, Phys. Rev. D **53**, 2442 (1996).

[29] L. Lavoura, Eur. Phys. J. C **29**, 191 (2003).

[30] A. Belyaev, C. Leroy, R. Mehdiyev, and A. Pukhov, JHEP **0509**, 005 (2005).

[31] J. Alwall *et al.*, Eur. Phys. J. C **49**, 791 (2007).

[32] G. C. Branco, P. A. Parada, and M. N. Rebelo, Phys. Rev. D **52**, 4217 (1995); E. Golowich, J. A. Hewett, S. Pakvasa, and A. A. Petrov, Phys. Rev. D **76**, 095009 (2007).

[33] M. Bona *et al.* [UTfit Collaboration], JHEP **0803**, 049 (2008).

[34] T. Aaltonen *et al.* [CDF Collaboration], Phys. Rev. Lett. **107**, 191801 (2011).

[35] R. Aaij *et al.* [LHCb Collaboration], arXiv:1112.1600.

[36] A. Dighe, A. Kundu, and S. Nandi, Phys. Rev. D **82**, 031502 (2010); A. Dighe, A. Kundu, and S. Nandi, Phys. Rev. D **76**, 054005 (2007).

[37] T. Inami and C. S. Lim, Prog. Theor. Phys. **65**, 297 (1981) [Erratum-ibid. **65**, 1772 (1981)].

[38] A. Soni, A. K. Alok, A. Giri, R. Mohanta, and S. Nandi, Phys. Rev. D **82**, 033009 (2010).

[39] Z. Ligeti, M. Papucci, G. Perez, and J. Zupan, Phys. Rev. Lett. **105**, 131601 (2010).

[40] A. Lenz and U. Nierste, JHEP **0706**, 072 (2007).

[41] Y. Grossman, Y. Nir, and G. Raz, Phys. Rev. Lett. **97** (2006) 151801.

[42] T. Aaltonen *et al.* [CDF Collaboration], Phys. Rev. Lett. **100**, 161802 (2008).

[43] V. M. Abazov *et al.* [D0 Collaboration], Phys. Rev. Lett. **101**, 241801 (2008).

[44] D. Asner *et al.* [Heavy Flavor Averaging Group], arXiv:1010.1589 [hep-ex].

[45] M. Ciuchini, Unitarity Triangle Analysis: An Update, talk given at the "Third Workshop on Theory, Phenomenology and Experiments in Heavy Flavour Physics", held in Anacapri, Italy, July 5-7, 2010.

[46] G. D'Agostini, hep-ph/0107067.

[47] A. K. Alok, A. Dighe, and D. London, Phys. Rev. D **83**, 073008 (2011).

[48] M. Hirsch, H. V. Klapdor-Kleingrothaus, and S. G. Kovalenko, Phys. Lett. B **372**, 181 (1996) [Erratum-ibid. B **381**, 488 (1996)]; H. Päs, M. Hirsch, and H. V. Klapdor-Kleingrothaus, Phys. Lett. B **459**, 450 (1999).

[49] H. Päs, M. Hirsch, and H. V. Klapdor-Kleingrothaus, Phys. Lett. **B459**, 450 (1999).

[50] L. Baudis *et al.*, Phys. Lett. B **407**, 219 (1997).